Virology 277, 127–135 (2000)
doi:10.1006/viro.2000.0604, available online at http://www.idealibrary.com on IDEAL®

The Human T-Cell Leukemia Virus Type I (HTLV-I) X Region Encoded Protein p13^{II} Interacts with Cellular Proteins

Xiaohong Hou,* Shanon Foley,* Maria Cueto,† and Mary Ann Robinson*,[1]

*Laboratory of Immunogenetics, National Institute of Allergy and Infectious Diseases, Twinbrook II Facility, National Institutes of Health, 12441 Parklawn Drive, Rockville, Maryland 20852; and †Novartis Institute for Biomedical Research, Biomolecular Structure and Computing/CTA, 556 Morris Avenue, Summit, New Jersey 07901

Received May 4, 2000; returned to author for revision July 11, 2000; accepted August 20, 2000

Interactions between the Human T-cell leukemia virus type I (HTLV-I) gene product p13^{II} and cellular proteins were investigated using the yeast two-hybrid system. Variant forms of p13^{II} were derived from two HTLV-I molecular clones, K30p and K34p, that differ in both virus production and *in vivo* and *in vitro* infectivity. Two nucleotide differences between the p13 from K30p (p13K30) and K34p (p13K34) result in a Trp-Arg substitution at amino acid 17 and the truncation of the 25 carboxyl-terminal residues of p13K34. A cDNA library from an HTLV-I-infected rabbit T-cell line was screened with p13K30 and p13K34 as bait. Products of two cDNA clones, C44 and C254, interacted with p13K34 but not with p13K30. Interactions were further confirmed using the GST-fusion protein coprecipitation assay. Sequence analysis of C44 and C254 cDNA clones revealed similarities to members of the nucleoside monophosphate kinase superfamily and actin-binding protein 280, respectively. Further analysis of the function of these two proteins and the consequence of their interaction with p13 may help elucidate a role for p13 in virus production, infectivity, or the pathogenesis of HTLV-I.

INTRODUCTION

Infectious molecular clones of viruses have provided the means for gaining insights into the role of individual viral proteins in the infectious process and in viral pathogenesis. Two molecular clones of Human T-cell leukemia virus type I (HTLV-I), K30p and K34p, which differ by only 18 nucleotides, have different functional characteristics. K30p mediates persistent infection both *in vitro* and *in vivo,* whereas K34p causes only transient infection (Zhao *et al.,* 1995, 1996). K30p and K34p differ in LTR, gag, pol, and the X regions (Zhao *et al.,* 1993).

Transfections of chimeric clones produced by combining different regions of the two parental clones allowed investigations into the roles of selected regions of HTLV-I and revealed the importance of the X region. Introduction of both or either of the two X-region substitutions from K34p into K30p resulted in a clone that, upon transfection, produced significantly decreased levels of virus and transient rather than persistent infectivity (Kindt *et al.,* 1999). Transfection of the parental K30p but not K34p clone into a T-cell line resulted in the dephosphorlyation of Vav (Mahana *et al.,* 1998), a cellular protein in a cell signal transduction pathway. Vav phosphorylation was downregulated in the cell line when transfected with a clone of K34p that contained both of the K30 pX substitutions, although the phosphorylation status of Vav was not altered if the chimeric clone contained only individual pX substitutions.

The HTLV-I X region consists of four open reading frames (ORFs) (Seiki *et al.,* 1983) and encodes at least six proteins (Koralnik *et al.,* 1992; Ciminale *et al.,* 1992; Kiyokawa *et al.,* 1985; Hidaka *et al.,* 1988; Sodroski *et al.,* 1984; Felber *et al.,* 1985). The two nucleotide differences between K30p and K34p located within the X region simultaneously result in amino acid differences in *rex,* p13^{II}, and p30^{II}. Therefore, the above-cited studies of molecular clones K30p, K34p, and chimeric clones constructed from them indicate that sequence differences in *rex,* p30^{II}, and/or p13^{II} products influence viral infectivity, the level of virus production, and Vav dephosphorylation within an infected cell.

The present study focuses on p13^{II} because there is little information concerning the function of p13^{II} and because p13^{II} represents the carboxyl-terminus of p30^{II}. The deduced protein sequence of p13^{II} reveals no characteristic DNA-binding motifs and previous data show neither DNA binding nor transcriptional activity (Roithmann *et al.,* 1994). Recent studies showed that p13^{II} targets to the mitochondria and results in morphological alterations of the mitochondrial membrane (Ciminale *et al.,* 1999). Together these data suggest that p13^{II} functions indirectly by interacting with cellular processes. The purpose of these studies was to investigate interactions between p13^{II} and cellular proteins.

[1] To whom correspondence and reprint requests should be addressed. Fax: (301) 402-0259. E-mail: mr23k@nih.gov.

0042-6822/00 $35.00

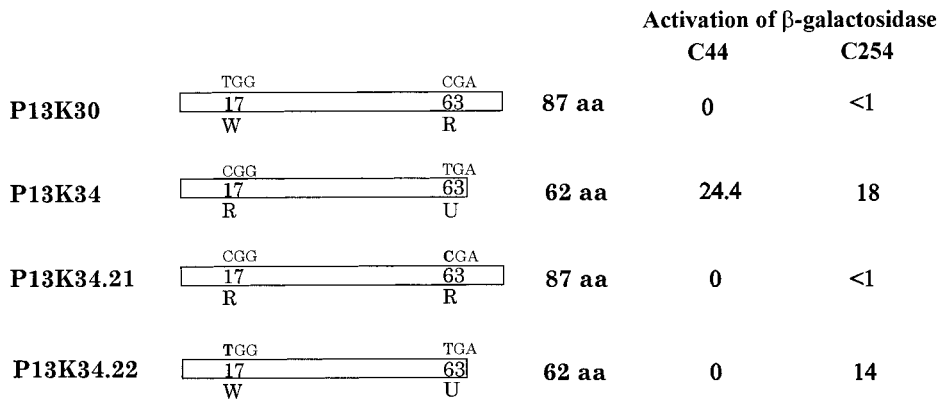

FIG. 1. Interaction of p13 variants with C44 and C254. Differences in the deduced protein sequences of p13K30, p13K34, and chimeric molecular clones, p13K34.21 and p13K34.22, are shown schematically. Numbers in the bars show the position of amino acid substitution with the nucleotide substitutions shown above. Amino acids are given using the single-letter code below the bar; U represents the stop codon. Interactions between the various forms of p13 with C44 and C254 were detected by quantitative liquid β-galactosidase assay after cotransforming the p13 containing DNA-binding plasmids and C44 or C254 containing DNA activation plasmid to yeast containing LacZ reporter gene. The numbers to the right represent fold activation of the β-galactosidase activity over background, which is the β-galactosidase activity detected in the yeast transformed by empty DNA-binding plasmid and DNA-activation plasmids. (GenBank accession no. for K30p, from which p13K30 was derived, is L03561; for K34p, from which p13K34 was derived, is L03562; for C44, AF195950; and for C254, AF244365).

RESULTS AND DISCUSSION

Isolation of clones encoding proteins that interact with p13^{II}

The yeast two-hybrid system (Ausubel *et al.,* 1994) was employed to identify intracellular proteins that interact with p13K30 and/or p13K34. Sequence differences between p13K30 and p13K34 include a replacement substitution of a Trp to an Arg at amino acid 17, introducing both a protein kinase C phosphorylation motif and a stop codon at position 63 of p13K34p (Fig. 1). Fusion proteins of p13K30 and p13K34 were expressed with the LexA DNA-binding domain. These constructs were used as bait to screen a cDNA library derived from the HTLV-I-infected rabbit T cell line, RH/K30, from which the molecular clone K30p was derived. A total of 1.3×10^8 clones were screened and 364 clones were selected for further investigation.

Two groups of clones, designated C44 and C254, were found to interact specifically with p13K34; no clones were isolated that interacted with p13K30. Cotransformation of yeast with p13K34 and C44 or C254 resulted in a 24- and 18-fold increase in β-galactosidase activity, respectively (Fig. 1). Cotransformation with the DNA-binding domain vector alone, the vector containing an irrelevant protein (bicoid), or p13K30 with either C44 or C254 failed to activate β-galactosidase activity (data not shown). These results indicate that the peptides encoded by C44 and C254 interact specifically with p13K34.

Chimeric molecular clones derived from p13K30 and p13K34 were used to identify the amino acids important in interactions with cellular proteins. Constructs containing all combinations of the two nucleotide substitutions in the p13^{II} between K30p and K34p were generated, as shown in Fig. 1. None of the chimeric clones encoded a protein that interacted with C44, indicating that neither the Trp at position 17 nor the C-terminal tail from p13K30 permitted interaction. In contrast, chimeric clone p13K34.22 encoded a protein that interacted with C254, indicating that the Trp at position 17 was compatible for the interaction but that the tail of p13K30 was not compatible for the interaction of p13 with C254.

The intact proteins encoded by both C44 and C254 were essential for interaction with p13K34. Constructs of C44 and C254 were produced by division of each into three segments (A, B, and C) based on domains of the molecules. Each of the three fragments and combinations of two fragments (AB and BC) were tested. Only the peptides encoded by the intact C44 and C254 cDNA interacted with p13K34 (data not shown).

Interactions between proteins identified using the yeast two-hybrid assay were further demonstrated by the ability of the p13^{II} variants to physically associate with GST-C44 and GST-C254 fusion proteins. Yeast strains containing bicoid, p13K30, p13K34, p13K34.21, and p13K34.22 constructs were lysed and confirmed for the expression of the relevant proteins by Western analysis, as shown in Fig. 2A. The yeast lysates were incubated with GST, GST-C44, or GST-C254 proteins bound to glutathione–Sepharose. The GST-C44 fusion protein did not interact with bicoid (data not shown), whereas it interacted with p13K30, p13K34, p13K34.21, and p13K34.22, even after washing in buffer with NaCl concentrations of up to 900 mM, suggesting strong molecular interactions (Fig. 2B). The discrepancy between *in vivo* and *in vitro* data indicates that there is a less-stringent requirement for interactions between p13 and C44 using this *in vitro* assay. All of the *in vivo* tests performed in the yeast two-hybrid system produced clear results for the functionally specific interaction between p13K34 and C44.

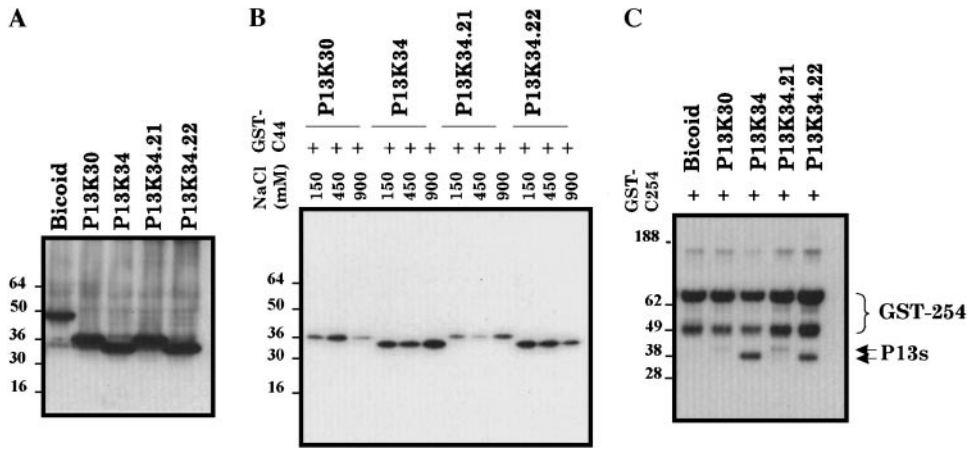

FIG. 2. Interaction of p13s with GST-C44 and GST-C254 *in vitro*. (A) Yeast strains containing bicoid, p13K30, p13K34, p13K34.21, and p13K34.22 in DNA-binding domain vector were lysed and the presence of these proteins in the lysate was confirmed by immunoblotting with anti-LexA antibody. The signal was detected by enhanced chemiluminescence. (B) Yeast lysates containing bicoid, p13K30, p13K34, p13K34.21, and p13K34.22 were incubated with GST or GST-C44 bound to glutathione–Sepharose matrix as indicated. The wash buffers contained a range of NaCl concentrations (150–900 mM) as indicated above the lanes. Proteins were separated by SDS–PAGE and transferred to a polyvinylidene difluoride membrane. The interaction of p13 and its variants with GST-44 was detected by immunoblotting using antibody to LexA and the signals were detected by enhanced chemiluminescence. (C) Yeast lysates containing bicoid, p13K30, p13K34, p13K34.21, and p13K34.22 were incubated with GST-C254 bound to glutathione–Sepharose matrix, separated by SDS–PAGE, and transferred to a polyvinylidene difluoride membrane. The membrane was blotted by antibody to GST and antibody to LexA and the signals were detected by enhanced chemiluminescence.

Both p13K34 and p13K34.22 interacted with GST-C254, whereas bicoid and p13K30 did not. P13K34.21 interacted with GST-254 very weakly (Fig. 2C). None of the p13II interacted with GST alone.

Characterization of C44

Sequence analysis of C44 revealed a deduced peptide sequence of 188 amino acids. BLAST analysis against the nonredundant protein database identified a human protein (Lai *et al.,* 2000) with 88% identity to the C44 sequence. Based on the high degree of conservation, this protein may represent the human homolog of C44. Additional cycles of PSI-BLAST (Altschul *et al.,* 1997) retrieved not only closely related hypothetical bacterial proteins but also more divergent members of the nucleoside monophosphate kinase (NMPK) superfamily (Fig. 3A). Frequently, the local pairwise alignments centered on the Gly-rich P-loop motif responsible for binding the phosphate groups of the NTP ligands.

To gain further insights into the biological function of C44, the complementary nature of four different computational sequence analysis algorithms were exploited. MAST searches (Henikoff *et al.,* 1995; Bailey and Gribskov, 1997) using C44-derived blocks retrieved several members of the NMPK superfamily, including eukaryotic, bacterial and archaeal adenylate, thymidylate, uridylate, and cytidylate kinases. These proteins represent the same matches found earlier using PSI-BLAST. In nearly all cases, the common conservation patterns are strongest around their respective nucleotide binding or P-loops. However, additional motifs, which are unique to the members of the archaeal adenylate kinases, are also present in C44. The approximate positions of these common motifs were verified using consensus-based secondary-structure prediction methods (Cuff *et al.,* 1998; Higgins *et al.,* 1996) and these sites are marked in Fig. 3A by a hatched line. C44 exhibited a similar organization of β-strands and α-helices as seen in the major secondary-structure elements of the crystal structure of the archaeal adenylate kinase (AK) from *Sulfolobus acidocaldarius,* suggesting a common topological fold. Moreover, the predicted molecular architecture of C44 contains key residues in common with the central β-sheet and the NTP-binding sites of members of the archaeal AK family. The α-helical regions in C44 are usually shorter than their counterparts in the archaeal AKs, and α-5 appears to be missing in C44, implying a more compact 3D structure.

Threading (Jones, 1999) also resulted in the retrieval of a number of NMPK 3D folds as the best ranking matches for both the rabbit and the human sequences. The strongest similarities among NMPK superfamily members surround the P loop that binds NTPs. The P-loop motif is quite ancient and conserved among NMPK superfamily members, yet other portions of the C44 molecule show greatest sequence similarities with the archaeal adenylate kinase rather than with members of a larger group of the NMPK family (Vonrhein *et al.,* 1998). The extent of similarities indicates that C44 is indeed evolutionarily related to the NMPK superfamily and may be able to bind NTPs via its P-loop motif. Whether C44 functions as an NMPK remains to be determined.

The expression of C44 mRNA was analyzed by Northern hybridization using a fragment of C44 as a probe.

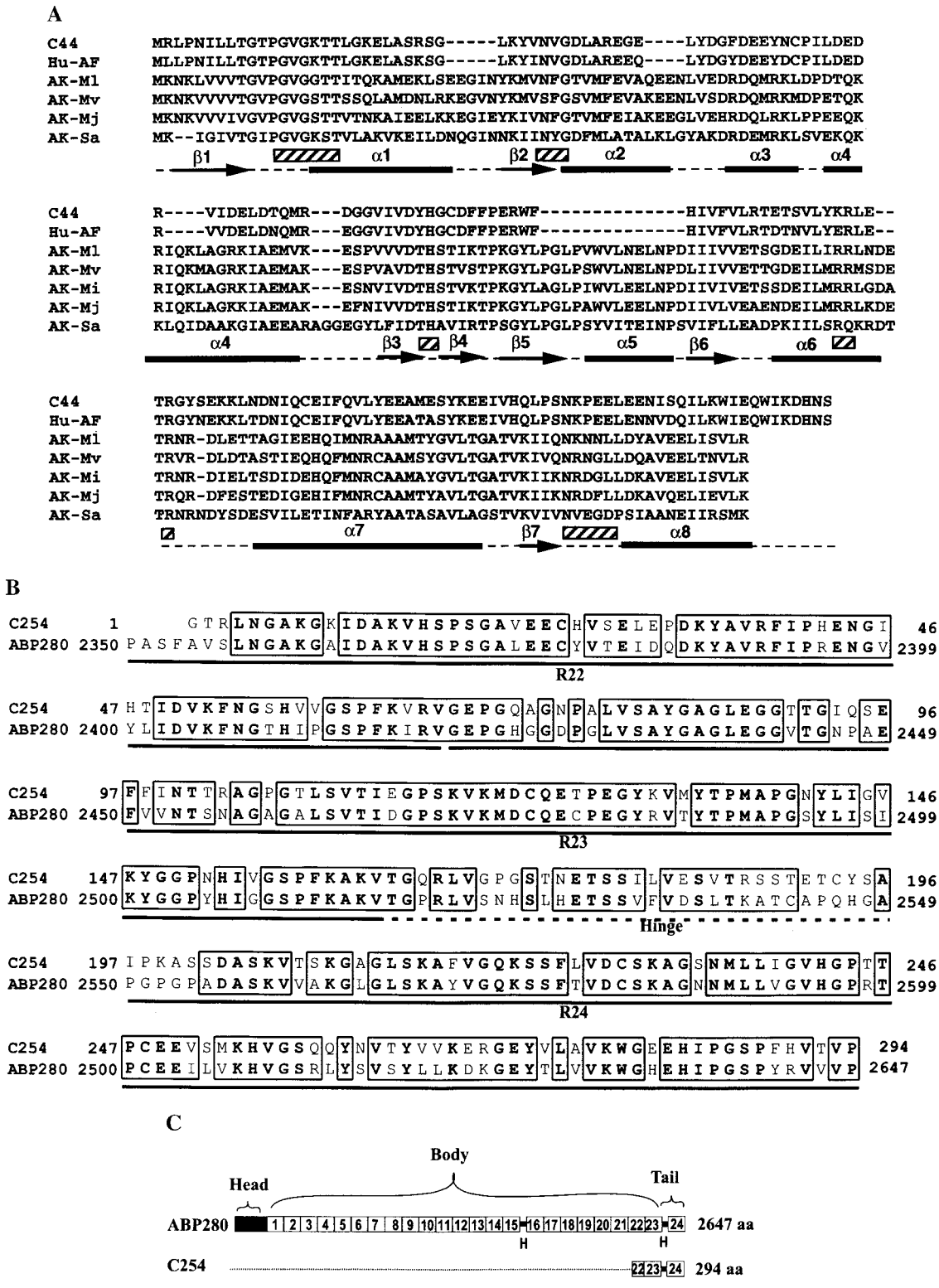

FIG. 3. Alignment of the deduced amino acid sequences of C44 and C254 with related proteins. (A) ClustalW multiple sequence alignment (MSA) of rabbit C44 sequence with human sequence (AF151895) and members of the archaeal adenylate kinase (AK) family from M. thermolithotrophicus (MI, U39880), M. voltae (Mv, U39879), M. igneus (Mi, U39881), M. jannaschii (Mj, U39882), and S. acidocaldarius (Sa, X73564). The organization of the secondary structure elements is shown below the sequence with β-strands shown as arrows and α-helices shown as heavy lines. Their approximate positions have been mapped onto the MSA using the crystal structure of S. acidocaldarius adenylate kinase (AK) as a template. A consensus approach based on complementary sequence analysis algorithms (i.e., PSI-BLAST, MAST, second-structure prediction methods, and threading) have confirmed the sequential organization of these structural elements on the amino acid sequence of C44. The nucleotide-binding motif or P-loop and other functionally important residues that are common to both C44 and AKs are marked below the sequence with a hatched line. (B) ClustalW

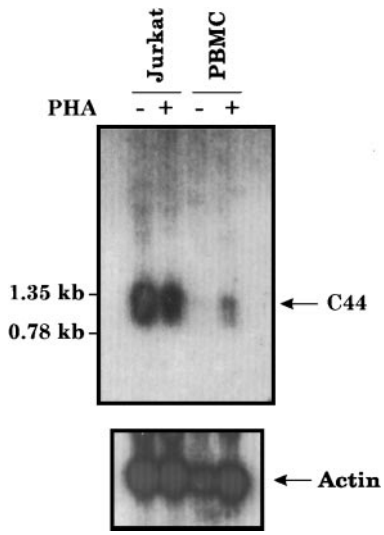

FIG. 4. Northern blot analysis of C44 mRNA. Autoradiogram of cellular RNA hybridized with radioactively labeled C44 probe. Approximately 10 μg of total RNA isolated from the indicated cells was separated on a 1% agarose/16% formaldehyde gel, transferred to a supported nitrocellulose membrane, and hybridized with an [α-^{32}P]dCTP-labeled 0.37-kb fragment from C44 cDNA. After a stringent wash, the blot was exposed for 2 days at −80°C (upper panel). The same blot was striped and rehybridized with an [α-^{32}P]dCTP-labeled human actin cDNA probe and exposed for 5 h at −80°C after wash (lower panel).

Jurkat cells and PBMC from a healthy donor were stimulated *in vitro* with PHA for 72 h prior to RNA extraction and the expression of C44 mRNA was compared with an equal amount of RNA from nonstimulated cells. Figure 4 shows that the C44 mRNA level is similar between stimulated and nonstimulated Jurkat cells, whereas C44 mRNA was detected only in stimulated PBMC but not in nonstimulated PBMC. No signal was detected in nonstimulated PBMC, even after longer exposure (data not shown). C44 mRNA was detected in human and rabbit transformed cell lines (data not shown). These results suggest that C44 mRNA is expressed in proliferating, but not resting, lymphoid cells.

Recently, Ciminale and coworkers (1999) showed that p13II localizes to mitochondria. Therefore, it is of great interest that C44 shows structural similarities to archaeal adenylate kinases, considering the evolutionary relationship between mitochondria and these ancient bacterial species (Lodish *et al.,* 2000). Furthermore, this previous study showed that in certain cells, p13II disrupted the mitochondrial membrane but did not appear to cause apoptosis (Ciminale *et al.,* 1999). The p13II used in these studies was most similar to p13K30, as it had the 25-amino-acid carboxyl tail. Based on the present study we predict that the p13II used by Ciminale *et al.* would not bind C44. The features of p13K34, but not p13K30, that allow the interaction with C44 may provide an additional signal that is required to effect apoptosis. Regulation of apoptosis is complicated and is likely to involve other HTLV-I and cellular factors.

Characterization of C254

The second clone found to interact with p13K34 was C254. The sequence of C254 was determined and compared with sequences in GenBank using BLAST. C254 encodes a 294-amino-acid peptide in a 0.88-kb ORF, which is followed by untranslated sequences and a polyA tail. The deduced amino acid sequence of C254 shows 69% identity and 83% similarity to the C-terminus of human nonmuscle filamin (actin-binding protein 280, ABP-280), with the alignment beginning at amino acid 2357 of ABP-280 (Fig. 3B). The full-length cDNA sequence of ABP-280 corresponds to a protein of 2647 amino acids consisting of three functional domains (Gorlin *et al.,* 1990). The N-terminal region serves as the actin-binding domain. The backbone contains 23 repeats, each about 96 residues long and the C-terminal tail consists of the 24th copy of the repeat sequence preceded by an inserted hinge region that serves as self-association domain. Clone C254 encodes a portion of repeat 22, all of repeat 23, the hinge sequence, and repeat 24 (Fig. 3C) at the C-terminal portion of the rabbit homolog of ABP-280.

The functional significance of this interaction is unclear but we hypothesize that binding of p13 to ABP280 alters its interaction with other cellular factors. ABP-280 is a prominent component present in the cytoskeleton of many different cell types (Gorlin *et al.,* 1990; Hartwig, 1994). ABP-280 functions in the modulation of cell shape and polarity and is essential for migration in melanocytes and other cultured cells (Cunningham *et al.,* 1992; Mitchison and Cramer, 1996; Drubin and Nelson, 1996). ABP-280 also plays a role in the insertion of adhesion molecules into the cell membrane (Meyer *et al.,* 1998). Several membrane receptors interact with different regions of ABP-280. The region of ABP-280 that interacts with p13K34 is also involved in interactions with integrin β1 (Loo *et al.,* 1998), tissue factor (Ott *et al.,* 1998), and presenilin (Zhang *et al.,* 1998), whereas other regions of the ABP-280 molecule are involved in the binding of glycoprotein ibα (Meyer *et al.,* 1997) and the cytoplasmic domain of furin (Liu *et al.,* 1997).

The interaction between p13K34 and ABP-280 may

sequence alignment of the peptide encoded by C254 with that of human nonmuscle filamin (ABP-280, GenBank accession no. 113001). Identical residues (in bold font) and similar residues (in regular font) are outlined. Repeated segments are identified and numbered under solid line and the hinge region is indicated by a dotted line under the sequence comparison. (C) Schematic representation of the portion of ABP-280 encoded by C254. Repeat segments are numbered and H indicates a hinge region.

impact several different features of HTLV-I infection and pathogenesis. Adhesion molecules play important roles in HTLV-I infections, including their involvement in the induction of T-cell activation (Buckle *et al.,* 1996) and in syncytium formation (Daenke *et al.,* 1999). Whether the interaction would enhance or disrupt normal cellular processes is unknown nor is it known whether ABP-280 impacts the expression of the relevant adhesion molecules. However, because the variant p13K34.22 (Fig. 1) is able to interact with C254, but not with C44, it is possible to investigate the impact of interactions with only C254.

Determination of whether the hypothesized effects of $p13^{II}$ are indeed associated with the virus clones (K30p, K34p) or with their parental cell lines (RH/K30, RH/K34) is precluded by the fact that the clone K34p from which p13K34 was derived does not cause persistent infection *in vitro* or *in vivo* (Zhao *et al.,* 1995, 1996). The present studies may reveal a reason why K34p fails to cause persistent infections: that is, it may induce apoptosis of the cells that it infects. Additional studies are required to establish whether p13K34 does cause apoptosis, yet the cell line RH/K34, from which the clone K34p derived, shows pathogenic features when injected into rabbits including apoptosis of T lymphocytes (Simpson *et al.,* 1996; Leno *et al.,* 1995).

In summary, the $p13^{II}$ from K34p was found to interact with two different cellular proteins that we have designated C44 and C254. C44 shows structural similarities to archaeal adenylate kinases, whereas C254 appears to be rabbit ABP-280. Possible impacts of these interactions include the induction of apoptosis and modulation of adhesion molecule insertion into the cell membrane. HTLV-I infection is associated with a variety of diseases, affecting only a small percentage of infected individuals. The genome of HTLV-I is complex and different viral products have different impacts on the host. Variation in individual viral products that can occur by mutation over the course of an HTLV-I infection may provide additional functions to HTLV-I products such as $p13^{II}$ that play important roles in virus production or in the pathogenesis of HTLV-I.

MATERIALS AND METHODS

Yeast two-hybrid system

Roger Brent, Department of Molecular Biology, Massachusetts General Hospital and Department of Genetics, Harvard Medical School, kindly provided the vectors and yeast strains used in the yeast two-hybrid system (Zervos *et al.,* 1993).

cDNA library

A cDNA library was prepared from RNA isolated from an HTLV-I-infected rabbit lymphocyte cell line, designated RH/K30. The library was constructed into the *Eco*RI–*Xho*I sites of the 2-μm *TRP1* galatose-inducible vector pJG4-5 that expresses individual cDNA as fusion proteins containing a transcription activation domain and influenza virus hemagglutinin epitope (Zervos *et al.,* 1993).

DNA-binding domain vectors

The p13 gene from K30p, K34p, and chimeras was constructed using PCR amplification and cloned downstream of the DNA-binding protein LexA in the *Eco*RI–*Bam*HI site of the 2-μm *HIS3* vector pEG202 (Zervos *et al.,* 1993). Yeast strain EGY48 (MATa, trp1 ura3 his3 LEU: pLexop6-LEU2) was transformed sequentially with pSH18-34 (URA3), which directs the expression of reporter genes leu2 and lacZ and the DNA-binding plasmid pEG202 containing p13, to produce the line used for transformation with the cDNA library.

cDNA library screening

The sequentially transformed yeast strain described above was transformed with the pJG4-5-based RH/K30 cDNA library by the lithium acetate method of Ito *et al.* (1983). The primary transformants from screening by p13K30 and from screening by p13K34 were collected from glucose/$Ura^-His^-Trp^-$ selection plates. An aliquot of the pooled transformants was spread on galactose/$Ura^-His^-Trp^-Leu^-$ plates and Leu-positive colonies were streaked onto glucose/$Ura^-His^-Trp^-$ master plates. Colonies from master plates were replicated onto four plates: glucose/X-gal (5-bromo-4-chloro-3-indodyl-β-D-galactopyranoside)/$Ura^-His^-Trp^-$; galactose/raffinose/X-gal/$Ura^-His^-Trp^-$; glucose/$Ura^-His^-Trp^-Leu^-$; and galactose/raffinose/$Ura^-His^-Trp^-Leu^-$. Plasmids from colonies that turned blue on the galactose/raffinose/X-gal/$Ura^-His^-Trp^-$ plate and grew on the galactose/raffinose/$Ura^-His^-Trp^-Leu^-$ plate were purified and cDNA clones were grouped based on restriction digestion pattern. One representative cDNA from each group was sequenced by Dye Terminator Cycle Sequencing system using an ABI 373 sequencer (Perkin Elmer/Applied Biosystems, Foster City, CA).

β-Galactosidase assay

Three independent colonies from each candidate transformant were taken for quantitative liquid β-gal assay. Yeast was grown overnight at 30°C in galactose and raffinose containing selection media. The cells were washed by ultrapure water and resuspended in Z buffer (10 mM KCl, 1 mM $MgSO_4$, 60 mM Na_2PO4, 40 mM NaH_2PO_4) to an optical density of 0.2 U/ml at 600 nm. Cells were permeabilized by adding 15 μl of 0.1% sodium dodecyl sulfate (SDS) and 20 μl of chloroform followed by vortexing for 10 s. After equilibrating samples at 30°C, 0.2 ml of *o*-nitrophenyl-β-D-galactoside (ONPG) at a concentration of 4 mg/ml in Z buffer was added. When a

medium-yellow color developed, the reaction was stopped by addition of 0.5 ml of 1 M Na_2CO_3. The cells were pelleted and the optical density at 420 nm of the supernatant was measured.

Database searches

Iterative database searches were performed with PSI-BLAST against nonredundant SwissProt sequences database (Altschul *et al.,* 1997). Currently no single computational methodology guarantees the optimal detection of all divergent members in protein families. Thus, to investigate a possible evolutionary connection between isolated clones and matches from GenBank, three additional complementary approaches were used. First, ungapped conserved regions (or blocks) and close homologs were converted to position-specific scoring matrices (PSSMs or profiles) using BlockMaker and subsequently submitted as probes in MAST searches (Henikoff *et al.,* 1995; Bailey and Gribskov, 1997). Second, a combination of secondary-structure prediction methods was used with multiple sequence alignments generated by ClustalW (Cuff *et al.,* 1998; Higgins *et al.,* 1996). In addition, a fold recognition method (GenThreader) that measures the compatibility of a primary sequence with a library of tertiary templates was applied (Jones, 1999).

Expression of GST fusion protein

PCR-amplified cDNA fragments from the cDNA library screening were inserted in frame into the polycloning site of pGEX-4T-3 (Amersham Pharmacia Biotech, Piscataway, NJ) downstream of the gene for glutathione-*S*-transferase (GST) and transformed into DH5α-competent cells (Life Technologies, Gaithersburg, MD). Expression of GST fusion proteins was induced by 0.1 mM of isopropyl-β-D-thiogalactoside (IPTG) for 1 h when bacterial growth reached the logarithmic stage in Luria–Bertani medium. The bacterial culture was harvested, washed, and lysed by incubating with 1 mg/ml of lysozyme for 30 min followed by sonication at 4°C in PBS containing protease inhibitor cocktail (1 tablet/10 ml; Roche Molecular Biochemicals, Indianapolis, IN). After centrifugation a portion of lysate was analyzed by SDS–PAGE and the expressions of GST and GST fusion protein were revealed by immunoblotting using an anti-GST antibody (Clontech, Palo Alto, CA).

In vitro binding assay and Western blot analysis

Glutathione–Sepharose 4B (Amersham Pharmacia Biotech) immobilized GST or GST fusion proteins were incubated with ~10 μg of p13 and its derivatives for 14 h at 4°C in binding buffer (0.1% Triton X-100, 20 mM HEPES, pH 7.5, 10% glycerol, and 150 mM NaCl). Samples of p13 were derived from the lysates of yeast containing the p13 DNA-binding constructs. After three washes in binding buffer, the beads were boiled for 5 min in SDS sample buffer including 5% 2-mecaptoethanol, 2 μg/ml each aprotinin, leupeptin, and 1 mM of phenylmethylsulfonyl fluoride (PMSF). Proteins were separated on a 10% NuPage gel or a 4–12% Tris–glycine gel (Novex, San Diego, CA) by electrophoresis and transferred to a polyvinylidene difluoride membrane. The membrane was blocked with blocking buffer (phosphate-buffered saline [PBS] containing 5% skim milk and 0.05% Tween 20) and incubated with mouse monoclonal antibody (MAb) to LexA (Clontech) at a dilution of 1: 5000 for 1 h. After rinsing for 30 min in PBS containing 0.05% Tween 20, the membrane was incubated with horseradish peroxidase-conjugated goat anti-mouse immunoglobulin (Bio-Rad, Richmond, CA) at 1:10,000 dilution. After washing for 30 min, the immune complexes were detected by enhanced chemiluminescence (Amersham Pharmacia Bioech).

The expression of ABP-280 was detected by immunoblotting as described above with MAb to filamin (MCA724; Serotec, Bicester, UK) at a 1:5000 dilution. Cells were lysed in buffer containing 0.1% Nonidet-P40, 2 mM $MgCl_2$, 0.7 mM dithiothreitol, 70 mM K_2HPO, 55 mM Tris, pH 7.8, and protease inhibitor cocktail tablet (Roche Molecular Biochemicals), and the proteins were separated on 4–12% Tris–glycine gel (Novex).

RNA extraction and Northern blot analysis

Total RNA was extracted from cultured cells using an RNA purification kit (Qiagen, Chatsworth, CA) followed by treatment with DNase I (Life Technologies) to digest the contaminating DNA in RNA samples. A 10-μg sample of RNA was separated on a 1% agarose/16% formaldehyde gel. The gel was incubated in 0.05 N NaOH for 20 min and in HOH for 5 min, followed by incubation in 20× SSC for 45 min. RNA samples were transferred to supported nitrocellulose membrane using a downward transfer system (Turboblotter; Schleicher & Schuell, Keene, NH) and hybridized with [α-^{32}P]dCTP-labeled probe at 42°C for ~16 h in hybridization solution (10% dextran sulfate, 40% formamide, 4× SSC, 6.6 mM Tris, pH 8.0, 0.83× Denhardt's solution, and 50 μg/ml denatured salmon sperm DNA). After hybridization, the membrane was washed twice with 2× SSC/0.1% SDS at room temperature, once each with 0.1× SSC/0.05% SDS at room temperature at 45°C, and then developed by autoradiography. The probe used to hybridize C44 is a fragment of C44 cDNA from nucleotide 1 to 372 and the probe used to hybridize C254 is a fragment of C254 from nucleotide 256 to 885. Human β-actin cDNA (Clontech) was used as control probe.

T-cell activation

Freshly isolated PBMC and Jurkat cells (5×10^6) were incubated with 4 μg/ml of phytohemagglutinin (PHA) in 4 ml of complete RPMI (RPMI 1640 supplemented with penicillin at 100 U/ml, streptomycin at 100 μg/ml, 5 mM of

glutamine, and 10% fetal bovine serum) at 37°C in a humid incubator supplemented by 5% CO_2. The cells were collected at 72 h and RNA was extracted for Northern blot analysis as described above.

ACKNOWLEDGMENTS

We thank Dr. Roger Brent, Harvard Medical School, for providing the vectors and yeast strains used in the yeast two-hybrid system and Drs. V. M. Hirsch, A. A. Ansari, T. J. Kindt, and K.-T. Jeang (NIH) for critical review of the manuscript. Helpful suggestions from Drs. W. Mahana (NIH) and K. E. Clements (George Washington University) are gratefully acknowledged. We appreciate the excellent technical assistance of F. S. Bowers and editorial assistance of N. Cogan.

REFERENCES

Altschul, S. F., Madden, T. L., Schaffer, A. A., Zhang, J., Zhang, Z., Miller, W., and Lipman, D. J.(1997). Gapped BLAST and PSI-BLAST: A new generation of protein database search programs. *Nucleic Acids Res.* **25,** 3389–3402.

Ausubel, F. M., Brent, R., Kingston, R. E., Moore, D. D., Seidman, J. G., Smith, J. A., and Struhl, K. (1994). "Current Protocols in Molecular Biology." Wiley, New York.

Bailey, T. L., and Gribskov, M. (1997). Score distributions for simultaneous matching to multiple motifs. *J. Comput. Biol.* **4,** 45–59.

Buckle, G. J., Hafler, D. A., and Hollsberg, P. (1996). HTLV-I-induced T-cell activation. *J. Acquir. Immune Defic. Syndr. Hum. Retrovirol.* **13**(Suppl. 1), S107–S113.

Ciminale, V., Pavlakis, G. N., Derse, D., Cunningham, C. P., and Felber, B. (1992). Complex splicing in the human T-cell leukemia virus (HTLV) family of retroviruses: Novel mRNAs and proteins produced by HTLV type I. *J. Virol.* **66,** 1737–1745.

Ciminale, V., Zotti, L., D'Agostino, D. M., Ferro, T., Casareto, L., Franchini, G., Bernardi, P., and Chieco-Bianchi, L. (1999). Mitochondrial targeting of the p13II protein coded by the x-II ORF of human T-cell leukemia/lymphotropic virus type I (HTLV-I). *Oncogene* **18,** 4505–4514.

Cuff, J. A., Clamp, M. E., Siddiqui, A. S., Finlay, M., and Barton, G. J. (1998). JPred: A consensus secondary structure prediction server. *Bioinformatics* **14,** 892–893.

Cunningham, C. C., Gorlin, J. B., Kwiatkowski, D. J., Hartwig, J. H., Janmey, P. A., Byers, H. R., and Stossel, T. P. (1992). Actin-binding protein requirement for cortical stability and efficient locomotion. *Science* **255,** 325–327.

Daenke, S., McCracken, S. A., and Booth, S. (1999). Human T-cell leukaemia/lymphoma virus type 1 syncytium formation is regulated in a cell-specific manner by ICAM-1, ICAM-3 and VCAM-1 and can be inhibited by antibodies to integrin beta2 or beta7. *J. Gen. Virol.* **80,** 1429–1436.

Drubin, D. G., and Nelson, W. J. (1996). Origins of cell polarity. *Cell* **84,** 335–344.

Felber, B. K., Paskalis, H., Kleinman-Ewing, C., Wong-Staal, F., and Pavlakis, G. N. (1985). The pX protein of HTLV-I is a transcriptional activator of its long terminal repeats. *Science* **229,** 675–679.

Gorlin, J. B., Yamin, R., Egan, S., Stewart, M., Stossel, T. P., Kwiatkowski, D. J., and Hartwig, J. H. (1990). Human endothelial actin-binding protein (ABP-280, nonmuscle filamin): A molecular leaf spring. *J. Cell Biol.* **111,** 1089–1105.

Hartwig, J. H. (1994). Actin-binding proteins 1: Spectrin superfamily. *Protein Profile* **1,** 706–778.

Henikoff, S., Henikoff, J. G., Alford, W. J., and Pietrokovski, S. (1995). Automated construction and graphical presentation of protein blocks from unaligned sequences. *Gene* **163,** GC17–GC26.

Hidaka, M., Inoue, J., Yoshida, M., and Seiki, M. (1988). Post-transcriptional regulator (rex) of HTLV-1 initiates expression of viral structural proteins but suppresses expression of regulatory proteins. *EMBO J.* **7,** 519–523.

Higgins, D. G., Thompson, J. D., and Gibson, T. J. (1996). Using CLUSTAL for multiple sequence alignments. *Methods Enzymol.* **266,** 383–402.

Ito, H., Fukuda, Y., Murata, K., and Kimura, A. (1983). Transformation of intact yeast cells treated with alkali cations. *J. Bacteriol.* **153,** 163–168.

Jones, D. T. (1999). GenTHREADER: An efficient and reliable protein fold recognition method for genomic sequences. *J. Mol. Biol.* **287,** 797–815.

Kindt, T. J., Zhao, T., Simpson, R. M., Hague, B. S., Robinson, M. A., and Mahana, W. (1999). "Molecular Pathogenesis of HTLV-1: A Current Perspective" (O. J. Semmes and M.-L. Hammarskjold, Eds.). ABI Professional Publications, Arlington, VA.

Kiyokawa, T., Seiki, M., Iwashita, S., Imagawa, K., Shimizu, F., and Yoshida, M. (1985). p27x-III and p21x-III, proteins encoded by the pX sequence of human T- cell leukemia virus type I. *Proc. Natl. Acad. Sci. USA* **82,** 8359–8363.

Koralnik, I. J., Gessain, A., Klotman, M. E., Monico, A. L., Berneman, Z. N., and Franchini, G. (1992). Protein isoforms encoded by the pX region of human T-cell leukemia/lymphotropic virus type I. *Proc. Natl. Acad. Sci. USA* **89,** 8813–8817.

Lai, C. H., Chou, C. Y., Ch'ang, L. Y., Liu, C. S., and Lin, W. (2000). Identification of novel human genes evolutionarily conserved in caenorhabditis elegans by comparative proteomics [In Process Citation]. *Genome Res.* **10,** 703–713.

Leno, M., Simpson, R. M., Bowers, F. S., and Kindt, T. J. (1995). Human T lymphocyte virus 1 from a leukemogenic cell line mediates in vivo and in vitro lymphocyte apoptosis. *J. Exp. Med.* **181,** 1575–1580.

Liu, G., Thomas, L., Warren, R. A., Enns, C. A., Cunningham, C. C., Hartwig, J. H., and Thomas, G. (1997). Cytoskeletal protein ABP-280 directs the intracellular trafficking of furin and modulates proprotein processing in the endocytic pathway. *J. Cell Biol.* **139,** 1719–1733.

Lodish, H., Berk, A., Zipursky, S. L., Matsudaira, P., Baltimore, D., and Darnell, J. (2000). "Molecular Cell Biology," 4 ed. W. H. Freeman, New York.

Loo, D. T., Kanner, S. B., and Aruffo, A. (1998). Filamin binds to the cytoplasmic domain of the beta1-integrin: Identification of amino acids responsible for this interaction. *J. Biol. Chem.* **273,** 23304–23312.

Mahana, W., Zhao, T. M., Teller, R., Robinson, M. A., and Kint, T. J. (1998). Genes in the pX region of human T cell leukemia virus I influence Vav phosphorylation in T cells. *Proc. Natl. Acad. Sci. USA* **95,** 1782–1787.

Meyer, S. C., Sanan, D. A., and Fox, J. E. (1998). Role of actin-binding protein in insertion of adhesion receptors into the membrane. *J. Biol. Chem.* **273,** 3013–3020.

Meyer, S. C., Zuerbig, S., Cunningham, C. C., Hartwig, J. H., Bissell, T., Gardner, K., and Fox, J. E. (1997). Identification of the region in actin-binding protein that binds to the cytoplasmic domain of glycoprotein IBalpha. *J. Biol. Chem.* **272,** 2914–2919.

Mitchison, T. J., and Cramer, L. P. (1996). Actin-based cell motility and cell locomotion. *Cell* **84,** 371–379.

Ott, I., Fischer, E. G., Miyagi, Y., Mueller, B. M., and Ruf, W. (1998). A role for tissue factor in cell adhesion and migration mediated by interaction with actin-binding protein 280. *J. Cell Biol.* **140,** 1241–1253.

Roithmann, S., Pique, C., Cesne, A. L., Delamarre, L., Pham, D., Tursz, T., and Dokhelar, M.-C. (1994). The open reading frame I (ORFI)/ORFII part of the human T-cell leukemia virus type I X region is dispensable for $p40^{tax}$, $p27^{rex}$, or envelope expression. *J. Virol.* **68,** 3448–3451.

Seiki, M., Hattori, S., Hirayama, Y., and Yoshida, M. (1983). Human adult T-cell leukemia virus: Complete nucleotide sequence of the provirus genome integrated in leukemia cell DNA. *Proc. Natl. Acad. Sci. USA* **80,** 3618–3622.

Simpson, R. M., Zhao, T. M., Hubbard, B. S., Sawasdikosol, S., and Kindt,

T. J. (1996). Experimental acute adult T cell leukemia-lymphoma is associated with thymic atrophy in human T cell leukemia virus type I infection. *Lab. Invest.* **74,** 696–710.

Sodroski, J. G., Rosen, C. A., and Haseltine, W. A. (1984). Trans-acting transcriptional activation of the long terminal repeat of human T lymphotropic viruses in infected cells. *Science* **225,** 381–385.

Vonrhein, C., Bonisch, H., Schafer, G., and Schulz, G. E. (1998). The structure of a trimeric archaeal adenylate kinase. *J. Mol. Biol.* **282,** 167–179.

Zervos, A. S., Gyuris, J., and Brent, R. (1993). Mxi1, a protein that specifically interacts with Max to bind Myc-Max recognition sites [published erratum appears in Cell 1994 Oct 21;79(2):following 388]. *Cell* **72,** 223–232.

Zhang, W., Han, S. W., McKeel, D. W., Goate, A., and Wu, J. Y. (1998). Interaction of presenilins with the filamin family of actin-binding proteins. *J. Neurosci.* **18,** 914–922.

Zhao, T. M., Robinson, M. A., Bowers, F. S., and Kindt, T. J. (1995). Characterization of an infectious molecular clone of human T-cell leukemia virus type I. *J. Virol.* **69,** 2024–2030.

Zhao, T. M., Robinson, M. A., Bowers, F. S., and Kindt, T. J. (1996). Infectivity of chimeric T-cell leukemia virus type I molecular clones assessed by naked DNA inoculation. *Proc. Natl. Acad. Sci. USA* **93,** 6653–6658.

Zhao, T. M., Robinson, M. A., Sawasdikosol, S., Simpson, R. M., and Kindt, T. J. (1993). Variation in HTLV-I sequences from rabbit cell lines with diverse in vivo effects. *Virology* **195,** 271–274.